Current Biology 24, 1880–1886, August 18, 2014 ©2014 Elsevier Ltd All rights reserved http://dx.doi.org/10.1016/j.cub.2014.06.061

Report

Repeated Evolutionary Changes of Leaf Morphology Caused by Mutations to a Homeobox Gene

Adrien Sicard,[1] Anna Thamm,[1,4] Cindy Marona,[1] Young Wha Lee,[2] Vanessa Wahl,[3] John R. Stinchcombe,[2] Stephen I. Wright,[2] Christian Kappel,[1] and Michael Lenhard[1,*]

[1]Institut für Biochemie und Biologie, Universität Potsdam, Karl-Liebknecht Straße 24-25, 14476 Potsdam-Golm, Germany

[2]Department of Ecology & Evolutionary Biology, University of Toronto, 25 Willcocks Street, Toronto, ON M5S 3B2, Canada

[3]Department of Metabolic Networks, Max Planck Institute of Molecular Plant Physiology, Am Mühlenberg 1, 14476 Potsdam, Germany

Summary

Elucidating the genetic basis of morphological changes in evolution remains a major challenge in biology [1–3]. Repeated independent trait changes are of particular interest because they can indicate adaptation in different lineages or genetic and developmental constraints on generating morphological variation [4–6]. In animals, changes to "hot spot" genes with minimal pleiotropy and large phenotypic effects underlie many cases of repeated morphological transitions [4–8]. By contrast, only few such genes have been identified from plants [8–11], limiting cross-kingdom comparisons of the principles of morphological evolution. Here, we demonstrate that the *REDUCED COMPLEXITY* (*RCO*) locus [12] underlies more than one naturally evolved change in leaf shape in the Brassicaceae. We show that the difference in leaf margin dissection between the sister species *Capsella rubella* and *Capsella grandiflora* is caused by *cis*-regulatory variation in the homeobox gene *RCO-A*, which alters its activity in the developing lobes of the leaf. Population genetic analyses in the ancestral *C. grandiflora* indicate that the more-active *C. rubella* haplotype is derived from a now rare or lost *C. grandiflora* haplotype via additional mutations. In *Arabidopsis thaliana*, the deletion of the *RCO-A* and *RCO-B* genes has contributed to its evolutionarily derived smooth leaf margin [12], suggesting the *RCO* locus as a candidate for an evolutionary hot spot. We also find that temperature-responsive expression of *RCO-A* can explain the phenotypic plasticity of leaf shape to ambient temperature in *Capsella*, suggesting a molecular basis for the well-known negative correlation between temperature and leaf margin dissection.

Results and Discussion

Genetic and Developmental Basis of Leaf Shape Variation in the Genus *Capsella*

A morphological trait that has changed repeatedly in plant evolution is the shape of leaves [13–15]. The dissection of the leaf margin can vary from smooth to serrated to increasingly deeply lobed. In the Brassicaceae, increased and decreased leaf margin dissection has evolved independently several times [16], with changes in the *SHOOTMERISTEMLESS* (*STM*) expression pattern and deletion of the novel homeobox gene *REDUCED COMPLEXITY* (*RCO*) implicated in the loss of lobes in *Arabidopsis thaliana* [12, 15]. Species within the genus *Capsella* (shepherd's purse) show considerable variation in leaf shape. Nine tested accessions of the outbreeding *Capsella grandiflora* formed less dissected leaf margins than most accessions of the recently derived selfing species *Capsella rubella* [17–19], as assessed by the dissection index (perimeter^2/[4π × area]) and principal component analysis on elliptic Fourier descriptors (EFD-PCA) of the leaf outlines (Figures 1A–1D; Figures S1A and S1B available online; detailed experimental procedures are provided in the Supplemental Experimental Procedures). The increased leaf margin dissection observed in *C. rubella* was due to more lobes per leaf and to deeper sinuses between the lobes (Figures 1A and S1A). During plant development, the dissection index increased after the juvenile-to-adult transition, which occurred with very similar timing around leaves 8–9 in the two species, as judged by the appearance of abaxial trichomes as a marker for adult leaves [20]; it then rose to two times higher maximal values in *C. rubella* than in *C. grandiflora* (Figures 1B and S1C).

We used a population of recombinant inbred lines (RILs) [21] from a cross of *C. grandiflora* accession *Cg926* and *C. rubella* accession *Cr1504* to map quantitative trait loci (QTLs) underlying the variation in leaf margin dissection. The parental strains recapitulate the morphological variation seen at the level of the two species (Figures 1B and 1D). This approach identified three significant QTLs on chromosomes 1, 2, and 6, explaining 17%, 9%, and 30% of the phenotypic variance (Figure 1E; Table S1). Introgressing the *C. grandiflora* allele at the strongest QTL on chromosome 6 into the *C. rubella* background to generate near isogenic lines (NILs) confirmed its effect on leaf shape. Leaf shape (as assessed by the dissection index and EFD-PCA) was very similar between the parental *C. grandiflora* accession and the NIL homozygous for the *C. grandiflora* allele (*NILgg*), and the same was true for the parental *C. rubella* accessions and the NIL homozygous for the *C. rubella* allele (*NILrr*) (Figures 1F and S1E). The *C. rubella* allele not only increased the depth of the sinuses between the lobes but also rendered the lobes more complex (Figure S1D), with no influence on the timing of the juvenile-to-adult transition (Figure 1C). Thus, despite detecting more than one QTL in the initial mapping, one major locus can explain most of the phenotypic variation in leaf shape between the two accessions.

The areas of the alpha shapes (the hulls around the leaf blade and petiole, including all serrations) of leaf 14 were indistinguishable between plants carrying the *C. rubella* or the *C. grandiflora* QTL alleles; by contrast, the actual area of leaf 14 was smaller in the former, indicating that the *C. rubella* allele at the QTL primarily inhibits outgrowth of the sinuses (Figure S2A). Consistent with an equal initiation of lobes, the expression and subcellular localization pattern of a *pAtPIN1::AtPIN1-GFP* reporter marking the auxin convergence point at

[4]Present address: Department of Plant Sciences, University of Oxford, South Parks Road, Oxford OX1 3RB, UK

*Correspondence: michael.lenhard@uni-potsdam.de

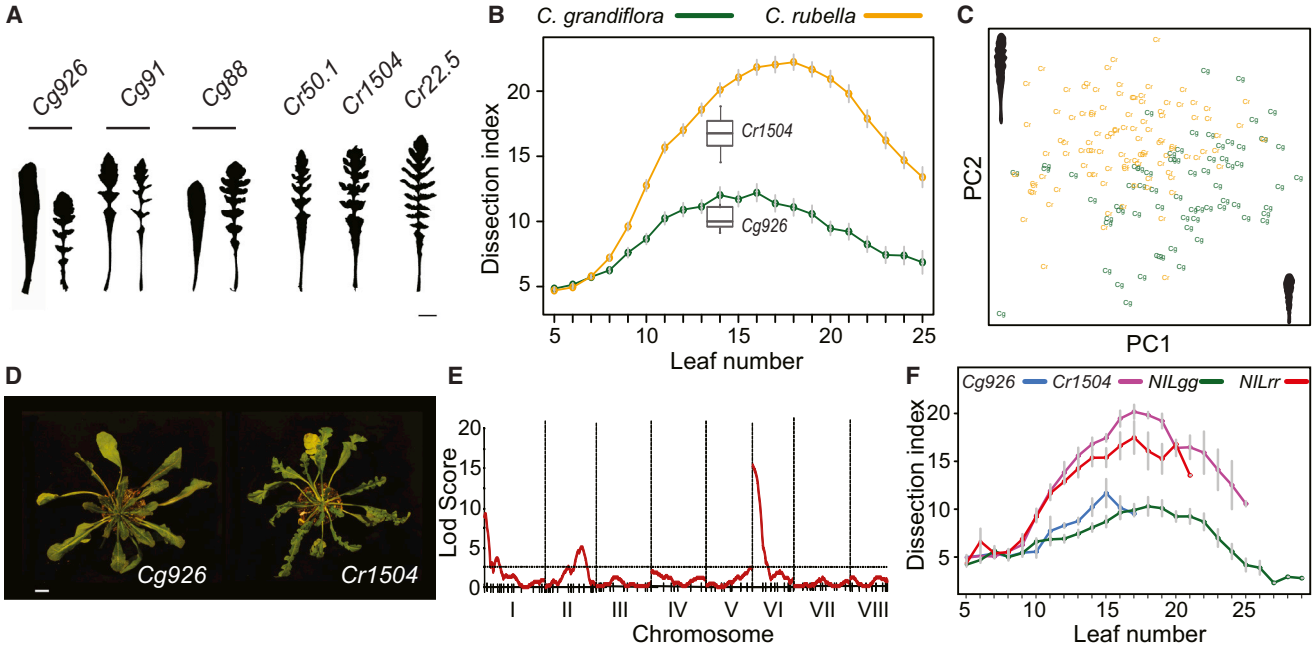

Figure 1. Leaf Shape Variation in *Capsella*

(A) Leaves from different *C. grandiflora* (*Cg*) and *C. rubella* (*Cr*) accessions. Leaves from two different individuals with extreme phenotypes are shown for each of the *Cg* accessions to illustrate within-accession variation.

(B) Dissection index of leaves averaged across *C. rubella* and *C. grandiflora* accessions. Values indicate mean ± SEM of 6 plants each of 9 *C. grandiflora* and 19 *C. rubella* accessions. Values for leaf 14 of the two RIL founders are shown. See Figure S1 legend for a definition of boxplots.

(C) EFD-PCA on *C. grandiflora* (green) and *C. rubella* (yellow) leaves. Each symbol represents a leaf 14.

(D) Whole-plant images of the RIL founders. Scale bar represents 1 cm.

(E) QTL mapping for leaf shape. Dashed horizontal line indicates 5% significance threshold.

(F) Dissection index of NILs and RIL founders. Values indicate mean ± SEM of six plants per genotype.

See also Figure S1.

the tips of leaf margin outgrowths [22, 23] was indistinguishable between both genotypes (Figure S2B). The CUP-SHAPED COTYLEDONS2 (CUC2) transcription factor inhibits outgrowth of the sinuses between *A. thaliana* leaf serrations [24]; similarly, overexpression of STM and BREVIPEDICELLUS (BP) causes leaf lobing in *A. thaliana* [25, 26]. Neither of these genes is upregulated in young leaves of *NILrr* versus *NILgg* plants (Figure S2C). Thus, the *C. rubella* allele at the QTL represses outgrowth of the sinuses, acting independently of known factors that increase leaf margin dissection.

Allelic Variation at *RCO-A* Underlies Leaf Shape Variation in *Capsella*

To isolate the causal gene, we phenotyped plants homozygous for recombinant chromosomes in the QTL interval using EFD-PCA (Figure S1F). From 1,500 plants, we identified two recombinant chromosomes that delimited a 110 kb interval containing the causal locus (Figure 2A; Table S2). Crossing the two recombinants yielded a quasi-isogenic line (qIL) segregating for this 110 kb interval but fixed for the flanking regions. The leaf dissection index of plants homozygous for the *C. rubella* allele (qILrr) was double that of plants homozygous for the *C. grandiflora* allele (qILgg), with no effect on the juvenile-to-adult transition (Figures 2B and S1C).

This interval in the *C. rubella* genome contains three tandemly duplicated, paralogous homeobox genes, termed *CrLMI1*, *CrRCO-A*, and *CrRCO-B* (Figure S2E). *CrLMI1* is the likely ortholog of *A. thaliana LATE MERISTEM IDENTITY1* (*LMI1*) [27], whose loss of function decreases leaf serration (Figure S2D); *CrRCO-A* and *CrRCO-B* encode proteins closely related to *Cardamine hirsuta* RCO [12] (Figures S4A and S5). The expression of *LMI1* and *RCO-A*, but not *RCO-B*, is higher in *NILrr* than *NILgg* plants, with *RCO-A* showing the most pronounced difference (Figures 2C and S2F). The difference in *RCO-A* expression was also evident by RNA in situ hybridization, demonstrating strong expression of *CrRCO-A* in a very localized group of subepidermal cells at the proximal flank of the emerging lobe, whereas *CgRCO-A* expression was virtually undetectable (Figures 2D–2F and S2H). Because only a genomic copy of the *CrRCO-A*, but not the *CrLMI1*, allele could cause leaf lobing in *A. thaliana* (see below), we focused on *CrRCO-A* as the most likely candidate. Transforming genomic constructs of *CrRCO-A* and *CgRCO-A* into *NILgg* plants recapitulated the effect of the two QTL alleles, with transformants carrying the *C. rubella* allele showing higher *RCO-A* expression and stronger leaf margin dissection than transformants with the *C. grandiflora* allele (Figures 2G–2J and S2G). Across both groups of transformants, the dissection index correlated with *RCO-A* expression levels (Figure 2I). Thus, allelic variation at the *RCO-A* locus underlies differences in leaf margin dissection between *C. rubella* and *C. grandiflora*.

Differences in *RCO-A* Expression Levels Underlie Different Leaf Morphologies and Phenotypic Plasticity

We compared the sequence of *CrRCO-A* from accession *Cr1504* with two *CgRCO-A* alleles from *C. grandiflora* accession 926, one isolated from a bacterial artificial chromosome library and used for the transformation experiment and

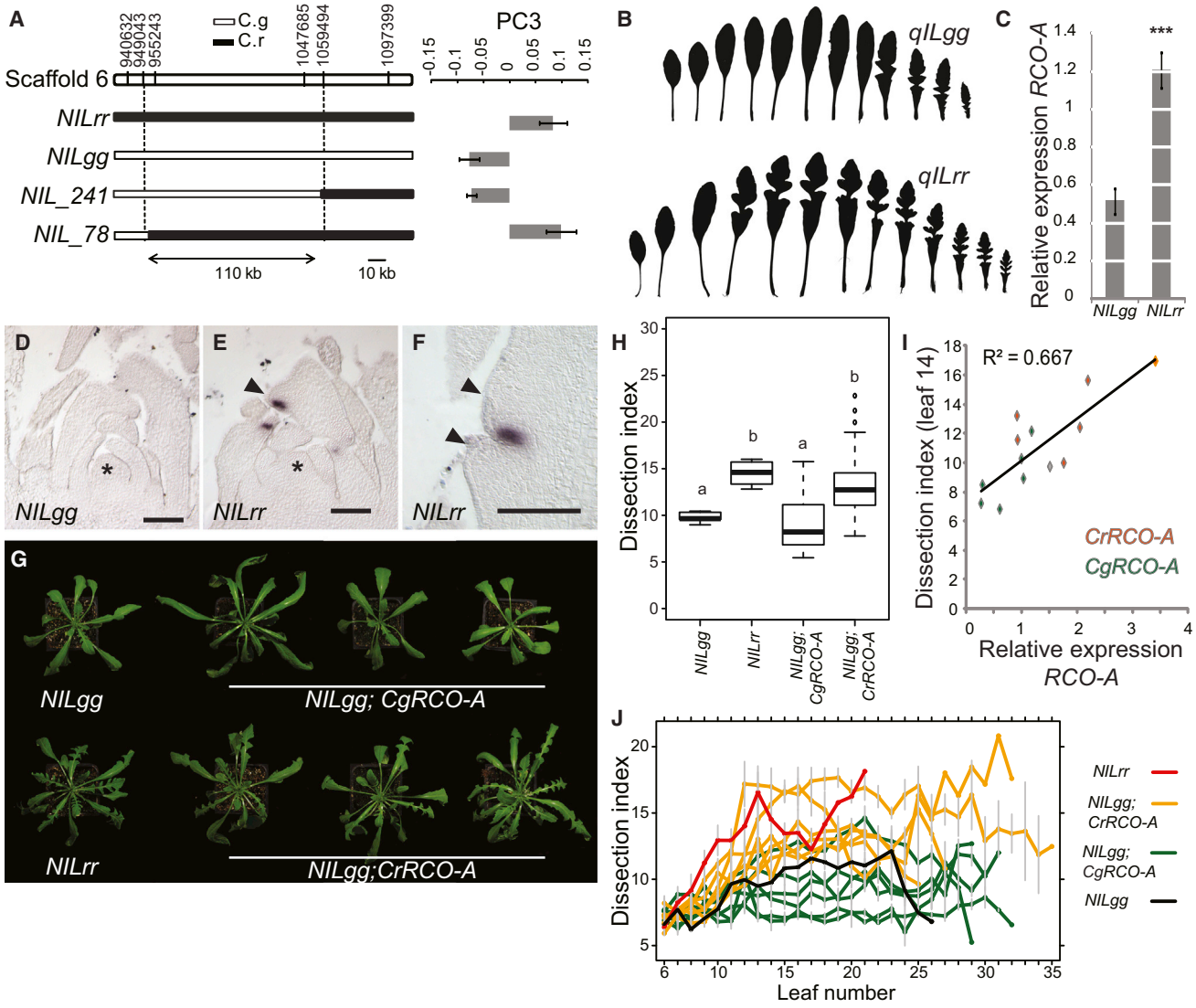

Figure 2. Allelic Variation in *RCO-A* Underlies Leaf Shape Differences

(A) Phenotypic effects of selected recombinant chromosomes. Boxes on the left indicate diploid genotypes of the four lines in question (empty: *C. grandiflora* homozygous; filled: *C. rubella* homozygous). For each line, bars on the right show the principal component 3 (PC3) values from PCA on EFDs of leaves from the fine-mapping population as a measure of leaf margin dissection. Each bar indicates the mean ± SEM of PC3 values for at least ten leaves per line. See Figure S1F for full EFD-PCR results from the fine-mapping population.

(B) Leaf outlines of plants from the qIL varying only in the 110 kb interval around the leaf shape QTL.

(C) Relative expression levels of *RCO-A*, as determined by quantitative RT-PCR (qRT-PCR), normalized to *CrTUB6*. Values indicate mean ± SEM of three biological replicates. Asterisks: significantly different at ***$p < 0.001$.

(D–F) RNA in situ hybridization against *RCO-A* mRNA on *NILgg* (D) or *NILrr* (E and F) plants. Scale bars represent 100 μm. Asterisks indicate shoot apical meristem; arrowheads mark outgrowing lobes.

(G) Whole-plant images of transgenic *Capsella* plants and the two NILs.

(H) Dissection index for leaf 14. Values are from six plants for the NILs and from six plants each for six independent transformants with the two *RCO-A* alleles. Letters indicate significant differences as determined by Tukey's honestly significant difference test.

(I) Correlation between *RCO-A* expression and dissection index in transgenic *NILgg* plants. Values indicate means of three biological replicates (expression) and six leaves per line (dissection index). Orange labels represent transformants with *CrRCO-A*; green labels show transformants with *CgRCO-A*. The gray symbol represents the *NILgg* background line for the transformation experiment.

(J) Dissection index throughout plant development in the NILs and independent transformant lines for the two allelic versions of *RCO-A*. Values indicate mean ± SEM from six plants per genotype.

See also Figure S2.

the other segregating in the RIL population. Two nonsynonymous exchanges between the *C. rubella* and the two *C. grandiflora* alleles lead to nonconservative amino acid exchanges at the RCO-A N terminus outside of the homeodomain (Figure S5). Besides single-nucleotide and small insertion/deletion polymorphisms, the putative promoter from the transformed *CrRCO-A* allele contained three large insertions relative to both *C. grandiflora* alleles (Figures S3B and S5), showing similarity to fragments of DNA and retrotransposons. The two *C. grandiflora* alleles differed in 43

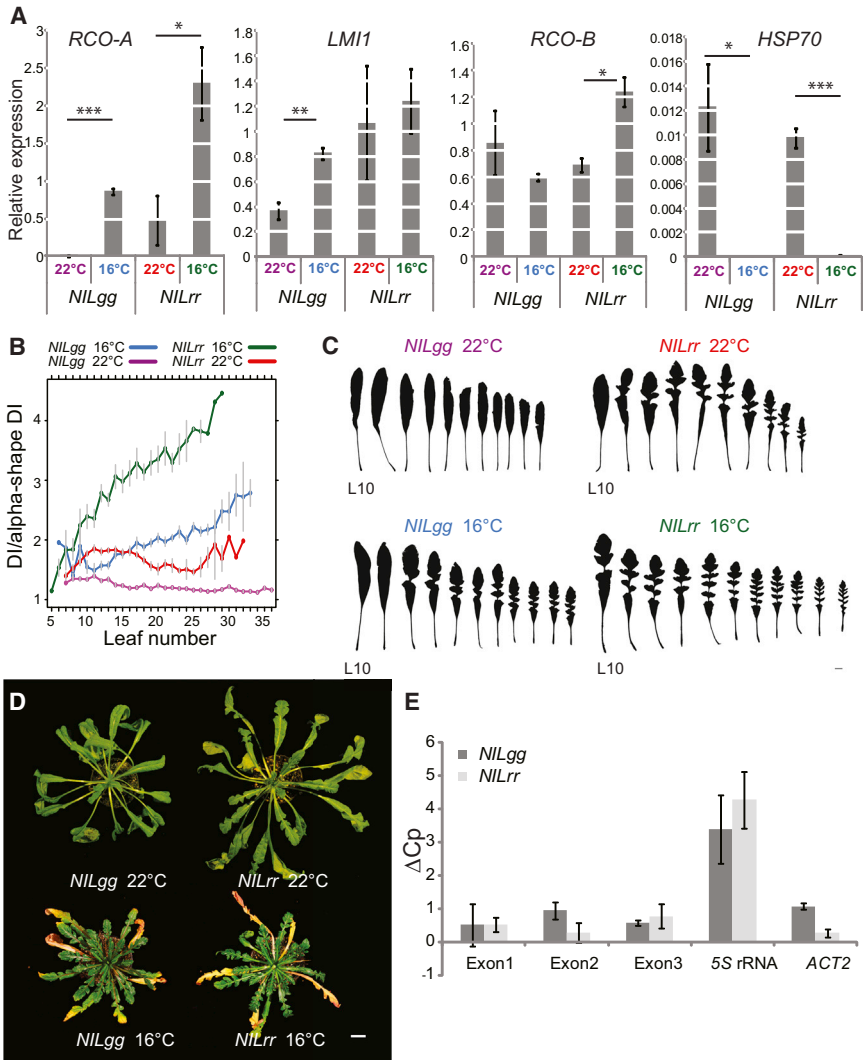

Figure 3. Phenotypic Plasticity Caused by Different *RCO-A* Allele Effects

(A) Relative expression levels of the indicated genes, as determined by qRT-PCR, normalized to *CrTUB6*. Values indicate mean ± SEM of three biological replicates. Asterisks: significantly different at *p < 0.05, **p < 0.01, and ***p < 0.001.
(B) Normalized dissection index (DI) of NIL plants grown at 16°C or at 22°C. Measured dissection indices were divided by dissection indices of alpha shapes for the leaves in order to account for temperature effects on overall leaf size and shape as evident in (D). For an unlobed leaf, this ratio is 1. Values indicate mean ± SEM for 15 plants each.
(C and D) Leaf outlines (C) and whole-plant images (D) of NIL plants grown at 16°C or at 22°C. L10, leaf 10; scale bar of (D) represents 1 cm.
(E) Methylation analysis using McrBC digestion. The ΔCp values of qPCR-amplification signal between undigested and McrBC-digested genomic DNA are shown for three regions in the *RCO-A* coding sequence and for two control regions, a hypomethylated (*ACT2*) and a hypermethylated (*5S* rRNA) region. The assay was performed on genomic DNA extracted from the apex of 15-day-old seedling grown at 22°C. Values indicate mean ± SEM of three biological replicates.

single-nucleotide and 8 small insertion/deletion polymorphisms in noncoding sequences.

To determine whether the different effects of the *RCO-A* alleles resulted from different protein activities due to the nonsynonymous polymorphisms in the coding sequence or from different expression levels, we exploited the temperature dependence of *RCO-A* expression (Figure 3). The *CgRCO-A* allele is upregulated more than 150-fold at 16°C compared to 22°C; for *CrRCO-A*, this upregulation was less than 5-fold (Figure 3A), whereas *LMI1* or *RCO-B* only responded to temperature in one, but not the other, genotype and did so more weakly than *RCO-A* (Figure 3A). Expression of the control gene *HSP70*, which has been shown to closely track ambient temperature in *A. thaliana* [28], was very similar between *NILgg* and *NILrr* plants grown at 16°C and between the two genotypes grown at 22°C, with a strong upregulation at 22°C (Figure 3A). This suggests that the different temperature responsiveness of the two *RCO-A* alleles does not result from an overall change in the temperature response between the two genotypes but rather reflects *cis*-regulatory variation at the locus. As a result of this, *CgRCO-A* expression in *NILgg* plants at 16°C was very similar to *CrRCO-A* expression in *NILrr* plants at 22°C. To be able to compare leaf margin dissection between the two conditions without the confounding effects of temperature on overall leaf shape and size (Figure 3D), we normalized the measured dissection index to that of the alpha shape of the leaf; for a smooth leaf margin, this ratio is 1. This normalized dissection index closely reflected *RCO-A* expression levels irrespective of genotype, being very similar between *NILgg* plants grown at 16°C and *NILrr* plants grown at 22°C (Figures 3B and 3C). Thus, we conclude that the two protein variants condition very similar leaf margin dissection when expressed at similar levels, indicating their functional equivalence. This in turn suggests *cis*-regulatory divergence as causing the different allele effects. *NILgg* plants showed a qualitative transition from entirely smooth leaf margins at 22°C to lobed leaves at 16°C; by contrast, *NILrr* leaves were lobed at both temperatures, with only a quantitative difference in the extent of lobing (Figures 3B and 3C). Thus, phenotypic plasticity of leaf shape is mediated by temperature-responsive *RCO-A* expression, and *cis*-regulatory variation between the alleles likely underlies their different phenotypic response to ambient temperature.

The expression differences between the two *RCO-A* alleles are reminiscent of a pattern that has recently emerged from genome-wide analyses in *A. thaliana* [29]. Whereas genes with comparatively higher gene body methylation show relatively high expression but reduced responsiveness to external stimuli (resembling the behavior of the *CrRCO-A* allele), genes with comparatively lower gene body methylation are more weakly expressed but respond more strongly to external changes (like *CgRCO-A*). We asked whether a higher gene body methylation in *CrRCO-A* as compared to *CgRCO-A* could contribute to the observed expression differences. Digestion of genomic DNA by the DNA methylation-dependent endonuclease McrBC followed by quantitative PCR [30] did not detect any difference

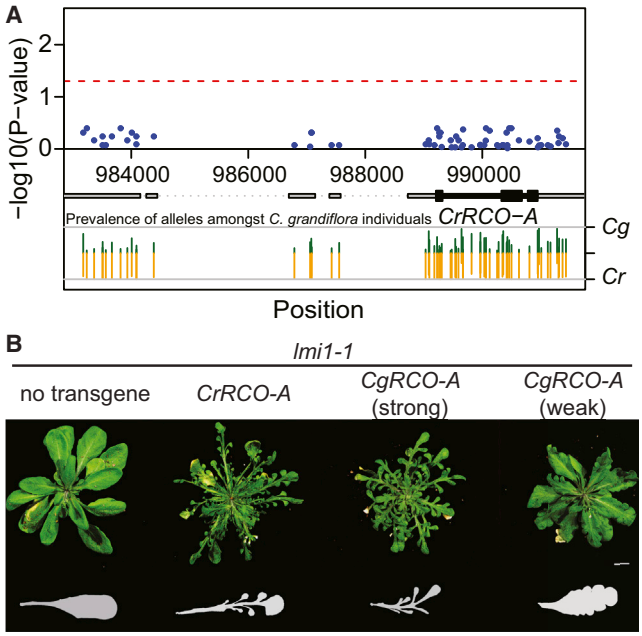

Figure 4. Repeated Mutations of *RCO* in Brassicaceae

(A) Local association mapping for leaf margin dissection in *C. grandiflora*. Gaps in gray bar indicate insertions in *C. rubella* reference genome. Dashed red line represents 5% significance threshold; p values were Benjamini-Hochberg corrected. Orange and green bars represent the frequency of analyzed *C. grandiflora* individuals carrying the *C. rubella*-like (orange) and the *C. grandiflora*-like (green) alleles at the respective positions. Sums over 100% are possible due to heterozygosity.

(B) Whole-plant images and leaf outlines of *A. thaliana lmi1-1* mutants transformed with *Capsella* alleles of *RCO-A*. Scale bar represents 1 cm.

See also Figures S3 and S4.

in methylation between the *CgRCO-A* and *CrRCO-A* coding sequences at all three tested positions (Figure 3E). Thus, the different temperature responsiveness and expression levels of the two alleles do not seem to reflect different methylation patterns.

Although the function of increased or reduced leaf margin dissection remains a matter of debate, dissection is known to be inversely correlated with mean annual temperature at the community and species levels; in fact, the degree of dissection in fossil leaves is widely used for paleoclimatic reconstructions [31–33]. To our knowledge, *RCO-A* is the first known factor that mediates between ambient temperature and leaf margin dissection, opening up the possibility of studying the relationship at the functional level.

Population Genetic Analysis of *RCO-A* in *Capsella*

We asked whether the variants in the *C. rubella* allele causing the higher dissection index had arisen by de novo mutations or had been captured from standing variation within the ancestral species *C. grandiflora*. To this end, we first sought to determine the allele frequency of the 64 SNPs and three large indel polymorphisms that differ between the transformed *Cr1504* and the *Cg926* alleles (Figure S5) in a sample of 188 resequenced *C. grandiflora* individuals from a population in Northern Greece and in a species-wide sample of 13 individuals (Figure S3A). Second, we performed local association mapping for leaf margin dissection using these polymorphisms. At 6 of 26 reliably genotyped SNPs in the promoter, one SNP in the first intron (990,275) and one of the large insertions (at 987,145), *C. rubella*-like alleles were virtually absent from *C. grandiflora* and found in only one of the 188 *C. grandiflora* individuals (107) and in two (or one) of the 13 species-wide individuals (93.2, 103.17; Figure S3A). Of the other two large insertions, one (at 987,580) was not present in any *C. grandiflora* sample, whereas the insertion at 984,156 was present in two of the species-wide *C. grandiflora* samples (93.2, 103.17; Figure S3A). Together with the observed variation in the large insertions among *C. rubella* accessions (Figures S3B–S3D), this indicates that these insertions are of relatively recent origin. Pairwise comparisons of haplotype blocks between *C. grandiflora* samples and *C. rubella* indicated that two of the three *C. grandiflora* samples with a *C. rubella*-like *RCO-A* haplotype (103.17, 107) show a higher proportion of *C. rubella*-like haplotypes across the genome or scaffold 6 than other, randomly selected *C. grandiflora* samples (Figure S3E); this suggests that they represent recent hybridization events. Because linkage disequilibrium decays within a few hundred base pairs in *C. grandiflora* (Figure S3F), the fact that all of the very rare *C. rubella*-like alleles spanning a more than 6 kb region are present in the same three *C. grandiflora* individuals also argues that this *C. rubella*-like haplotype was reintroduced into the *C. grandiflora* population by more recent hybridization rather than having been maintained as an unrecombined haplotype since before the split between the species about 50,000 to 100,000 years ago [34]. Three tests of neutrality (theta, Tajima's D, composite likelihood ratio test) all failed to find evidence for non-neutral evolution of the *RCO-A* locus in *C. grandiflora* (Table S3), suggesting that the locus is not experiencing positive or balancing selection in this species, consistent with the absence of common variants affecting leaf shape.

In the local association mapping, none of 90 SNPs in the *RCO-A* locus segregating among the 188 *C. grandiflora* individuals was significantly associated with leaf margin dissection (Figure 4A). Thus, together with the largely fixed phenotypic difference between the species, these findings argue that the *C. rubella* high-lobing allele was not captured from common standing variation in *C. grandiflora*; rather, it appears to have been derived from a now rare or lost *C. grandiflora* haplotype via insertions in the promoter. Variation in these insertions among *C. rubella* accessions suggests that some of them arose after the geographical spread of *C. rubella* following the divergence from *C. grandiflora* [18, 19]. Which of the insertions or neighboring SNP alleles cause the increased activity is unknown at present.

Loss of *RCO-A* Function in Brassicaceae Evolution

A. thaliana differs from its lobed-leafed relatives *Arabidopsis lyrata* and *Capsella* by having only minor serrations at the leaf base. This correlates with the deletion of the *RCO-A* and *RCO-B* orthologs in *A. thaliana* [12] (Figure S4A). Transforming genomic versions of *CrRCO-A* and *CgRCO-A*, but not *CrLMI1*, into *A. thaliana* is sufficient to restore the formation of lobes (Figures 4B and S4B), confirming a recent report [12]. To avoid interference with the endogenous activity of the sole member of the *LMI1/RCO* cluster in *A. thaliana*, we transformed the *Capsella* genomic constructs into the *A. thaliana lmi1-1* mutant. More than 50% of the *CrRCO-A* transformants showed increased leaf margin dissection, with some transformants forming deeply dissected leaves, and similar phenotypes were observed in the *CgRCO-A* transformants, albeit at a much lower frequency (Figures 4B and S4B). Again, the severity of the effect correlated with the expression strength of the transgene, independently of the protein variant (Figures 4B, S4C, and S4D), supporting

the conclusion that *cis*-regulatory variation at this locus underlies the leaf shape variation in *Capsella*.

Conclusions

Thus, independent *cis*-regulatory and deletion mutations targeting the cluster of *RCO* paralogs cause naturally occurring leaf shape changes in the Brassicaceae, suggesting *RCO* as a candidate for an evolutionary hot spot. *RCO* arose by duplication and gain of a divergent, highly specific expression pattern from an *LMI1*-like ancestral gene, while maintaining the same basic growth-repressing function and probably target genes [12]. It appears plausible that this evolutionary origin of *RCO* as a putative input/output gene [35] with spatially restricted expression mediating between upstream patterning factors and downstream targets underlies its suitability for evolutionary modification. This is because changes in its activity should be able to condition large phenotypic effects with little pleiotropy on other traits [6, 35]. As such, paralogs with divergent expression patterns and/or functions may be particularly amenable to evolutionary modification.

Accession Numbers

The NCBI GenBank accession numbers for the different *RCO-A* alleles from *C. grandiflora* reported in this paper are KM214233 and KM214234. The NCBI GenBank accession number for the *RCO-A* allele from *C. rubella* reported in this paper is KM214232. The NCBI SRA accession number for the *C. grandiflora* and *C. rubella* raw genome sequencing data is PRJNA255453.

Supplemental Information

Supplemental Information includes Supplemental Experimental Procedures, five figures, and three tables and can be found with this article online at http://dx.doi.org/10.1016/j.cub.2014.06.061.

Author Contributions

A.S. and M.L. designed the project. A.S., A.T., and C.M. performed QTL mapping, gene identification, phenotypic characterization, and transformation. A.S. and V.W. performed in situ hybridization. Y.W.L., J.R.S., and S.I.W. performed local association mapping and population genetic analyses. C.K. contributed to the population genetic analyses and carried out all other bioinformatic analyses. All authors analyzed data. S.I.W. and M.L. supervised the project. A.S. and M.L. wrote the manuscript, with input from all authors. All authors discussed and commented on the manuscript.

Acknowledgments

We thank Tanja Slotte and Barbara Neuffer for seeds; Doreen Mäker, Christiane Schmidt, and Monika Bischoff-Schäfer for excellent plant care; Mario Caccamo and The Genome Analysis Centre for resequencing the parental strains for the RIL population; and Isabel Bäurle and members of the M.L. group for discussion and comments on the manuscript. This work was supported by a Genome Canada and Genome Quebec Applied Bioproducts and Crops grant to S.I.W. and J.R.S. and by a European Research Council Starting Grant (260455) to M.L.

Received: May 14, 2014
Revised: June 24, 2014
Accepted: June 24, 2014
Published: August 7, 2014

References

1. Carroll, S.B. (2008). Evo-devo and an expanding evolutionary synthesis: a genetic theory of morphological evolution. Cell *134*, 25–36.
2. Stern, D.L., and Orgogozo, V. (2008). The loci of evolution: how predictable is genetic evolution? Evolution *62*, 2155–2177.
3. Hoekstra, H.E., and Coyne, J.A. (2007). The locus of evolution: evo devo and the genetics of adaptation. Evolution *61*, 995–1016.
4. Gompel, N., and Prud'homme, B. (2009). The causes of repeated genetic evolution. Dev. Biol. *332*, 36–47.
5. Losos, J.B. (2011). Convergence, adaptation, and constraint. Evolution *65*, 1827–1840.
6. Stern, D.L. (2013). The genetic causes of convergent evolution. Nat. Rev. Genet. *14*, 751–764.
7. Arendt, J., and Reznick, D. (2008). Convergence and parallelism reconsidered: what have we learned about the genetics of adaptation? Trends Ecol. Evol. *23*, 26–32.
8. Martin, A., and Orgogozo, V. (2013). The loci of repeated evolution: a catalog of genetic hotspots of phenotypic variation. Evolution *67*, 1235–1250.
9. Busch, A., and Zachgo, S. (2007). Control of corolla monosymmetry in the Brassicaceae Iberis amara. Proc. Natl. Acad. Sci. USA *104*, 16714–16719.
10. Cubas, P., Vincent, C., and Coen, E. (1999). An epigenetic mutation responsible for natural variation in floral symmetry. Nature *401*, 157–161.
11. Kim, M., Cui, M.L., Cubas, P., Gillies, A., Lee, K., Chapman, M.A., Abbott, R.J., and Coen, E. (2008). Regulatory genes control a key morphological and ecological trait transferred between species. Science *322*, 1116–1119.
12. Vlad, D., Kierzkowski, D., Rast, M.I., Vuolo, F., Dello Ioio, R., Galinha, C., Gan, X., Hajheidari, M., Hay, A., Smith, R.S., et al. (2014). Leaf shape evolution through duplication, regulatory diversification, and loss of a homeobox gene. Science *343*, 780–783.
13. Efroni, I., Eshed, Y., and Lifschitz, E. (2010). Morphogenesis of simple and compound leaves: a critical review. Plant Cell *22*, 1019–1032.
14. Koenig, D., and Sinha, N. (2010). Evolution of leaf shape: a pattern emerges. Curr. Top. Dev. Biol. *91*, 169–183.
15. Piazza, P., Bailey, C.D., Cartolano, M., Krieger, J., Cao, J., Ossowski, S., Schneeberger, K., He, F., de Meaux, J., Hall, N., et al. (2010). Arabidopsis thaliana leaf form evolved via loss of KNOX expression in leaves in association with a selective sweep. Curr. Biol. *20*, 2223–2228.
16. Al-Shehbaz, I.A., Beilstein, M.A., and Kellogg, E.A. (2006). Systematics and phylogeny of the Brassicaceae (Cruciferae): an overview. Plant Syst. Evol. *259*, 89–120.
17. Slotte, T., Hazzouri, K.M., Ågren, J.A., Koenig, D., Maumus, F., Guo, Y.L., Steige, K., Platts, A.E., Escobar, J.S., Newman, L.K., et al. (2013). The Capsella rubella genome and the genomic consequences of rapid mating system evolution. Nat. Genet. *45*, 831–835.
18. Foxe, J.P., Slotte, T., Stahl, E.A., Neuffer, B., Hurka, H., and Wright, S.I. (2009). Recent speciation associated with the evolution of selfing in *Capsella*. Proc. Natl. Acad. Sci. USA *106*, 5241–5245.
19. Guo, Y.L., Bechsgaard, J.S., Slotte, T., Neuffer, B., Lascoux, M., Weigel, D., and Schierup, M.H. (2009). Recent speciation of Capsella rubella from Capsella grandiflora, associated with loss of self-incompatibility and an extreme bottleneck. Proc. Natl. Acad. Sci. USA *106*, 5246–5251.
20. Telfer, A., and Poethig, R.S. (1998). HASTY: a gene that regulates the timing of shoot maturation in Arabidopsis thaliana. Development *125*, 1889–1898.
21. Sicard, A., Stacey, N., Hermann, K., Dessoly, J., Neuffer, B., Bäurle, I., and Lenhard, M. (2011). Genetics, evolution, and adaptive significance of the selfing syndrome in the genus Capsella. Plant Cell *23*, 3156–3171.
22. Barkoulas, M., Hay, A., Kougioumoutzi, E., and Tsiantis, M. (2008). A developmental framework for dissected leaf formation in the Arabidopsis relative Cardamine hirsuta. Nat. Genet. *40*, 1136–1141.
23. Bilsborough, G.D., Runions, A., Barkoulas, M., Jenkins, H.W., Hasson, A., Galinha, C., Laufs, P., Hay, A., Prusinkiewicz, P., and Tsiantis, M. (2011). Model for the regulation of Arabidopsis thaliana leaf margin development. Proc. Natl. Acad. Sci. USA *108*, 3424–3429.
24. Nikovics, K., Blein, T., Peaucelle, A., Ishida, T., Morin, H., Aida, M., and Laufs, P. (2006). The balance between the MIR164A and CUC2 genes controls leaf margin serration in Arabidopsis. Plant Cell *18*, 2929–2945.
25. Chuck, G., Lincoln, C., and Hake, S. (1996). KNAT1 induces lobed leaves with ectopic meristems when overexpressed in Arabidopsis. Plant Cell *8*, 1277–1289.
26. Lenhard, M., Jürgens, G., and Laux, T. (2002). The WUSCHEL and SHOOTMERISTEMLESS genes fulfil complementary roles in Arabidopsis shoot meristem regulation. Development *129*, 3195–3206.
27. Saddic, L.A., Huvermann, B., Bezhani, S., Su, Y., Winter, C.M., Kwon, C.S., Collum, R.P., and Wagner, D. (2006). The LEAFY target LMI1 is a meristem identity regulator and acts together with LEAFY to regulate expression of CAULIFLOWER. Development *133*, 1673–1682.

28. Kumar, S.V., and Wigge, P.A. (2010). H2A.Z-containing nucleosomes mediate the thermosensory response in Arabidopsis. Cell *140*, 136–147.
29. Coleman-Derr, D., and Zilberman, D. (2012). Deposition of histone variant H2A.Z within gene bodies regulates responsive genes. PLoS Genet. *8*, e1002988.
30. Pontier, D., Yahubyan, G., Vega, D., Bulski, A., Saez-Vasquez, J., Hakimi, M.-A., Lerbs-Mache, S., Colot, V., and Lagrange, T. (2005). Reinforcement of silencing at transposons and highly repeated sequences requires the concerted action of two distinct RNA polymerases IV in Arabidopsis. Genes Dev. *19*, 2030–2040.
31. Little, S.A., Kembel, S.W., and Wilf, P. (2010). Paleotemperature proxies from leaf fossils reinterpreted in light of evolutionary history. PLoS ONE *5*, e15161.
32. Royer, D.L., Wilf, P., Janesko, D.A., Kowalski, E.A., and Dilcher, D.L. (2005). Correlations of climate and plant ecology to leaf size and shape: potential proxies for the fossil record. Am. J. Bot. *92*, 1141–1151.
33. Royer, D.L., Meyerson, L.A., Robertson, K.M., and Adams, J.M. (2009). Phenotypic plasticity of leaf shape along a temperature gradient in Acer rubrum. PLoS ONE *4*, e7653.
34. Brandvain, Y., Slotte, T., Hazzouri, K.M., Wright, S.I., and Coop, G. (2013). Genomic identification of founding haplotypes reveals the history of the selfing species Capsella rubella. PLoS Genet. *9*, e1003754.
35. Davidson, E.H., and Erwin, D.H. (2006). Gene regulatory networks and the evolution of animal body plans. Science *311*, 796–800.